Available online at www.sciencedirect.com
SCIENCE DIRECT®
Journal of Computational Physics 207 (2005) 529–541
JOURNAL OF COMPUTATIONAL PHYSICS
www.elsevier.com/locate/jcp

A boundary integral formulation of quasi-steady fluid wetting

K.B. Glasner *

University of Arizona, Mathematics, 617 N Santa Rita, AZ 85721 Tucson, USA

Received 21 July 2004; received in revised form 13 January 2005; accepted 26 January 2005
Available online 3 March 2005

Abstract

This paper considers the motion of a liquid droplet on a solid surface. When capillary relaxation is much faster than the motion of the contact line, the fluid geometry and its dynamical evolution can be characterized in terms of the contact line alone. This problem can be cast in terms of boundary integral equations involving a Dirichlet–Neumann map coupled to a volume conservation constraint. A computational method for this formulation is described which has two principal advantages over approaches which track the entire free surface: (1) only the curve which describes the contact line is computed and (2) the resulting method exhibits only mild numerical stiffness, obviating the need for implicit time-stepping. Effects of both capillary and body forces are considered. Computational examples include surface inhomogeneities, topological transitions and cusp formation.

1. Introduction

Many practical applications involve the motion of a fluid over a solid surface. A large body of theory has emerged about the microscopic mechanisms which regulate the motion of the contact line [4,9,11,18,23,29,30,35,42], whereas less effort has been concentrated toward understanding the overall dynamics of wetting flows.

A typical approach to modeling wetting dynamics is the use of lubrication-type equations (e.g. [9,29]). While these models can incorporate numerous physical phenomenon, they suffer from several computational drawbacks. Capillary-driven motions necessarily lead to fourth order parabolic equations, which typically require expensive implicit algorithms. In addition, these equations are degenerate, and therefore require special treatment [17,43] to obtain sensible non-negative solutions (furthermore, the physical significance of these solutions is unclear because uniqueness has not been established). An alternative approach is

* Tel.: +1 520 621 4764.
E-mail address: kglasner@math.arizona.edu.

0021-9991/$ - see front matter © 2005 Elsevier Inc. All rights reserved.
doi:10.1016/j.jcp.2005.01.022

the use of disjoining pressure models [28,33,34], which can be well-posed but introduce a small horizontal length scale. As with diffuse interface methods [12], it is necessary to resolve this small scale numerically, leading to large grids or requiring adaptive mesh procedures.

A widely utilized class of macroscopic wetting models are laws which relate the speed of the contact line to other local properties of the fluid, in particular the "apparent" contact angle θ, the macroscopic angle which the fluid makes with the solid surface. For example, one of the most frequently cited empirical laws was introduced by Tanner [39],

$$V_c \sim \theta^3, \tag{1}$$

although many other formulas are available [4,7,10,41]. Laws like (1) may arise as leading-order approximations of the underlying dynamical equations [3,7,8,14,20,41], and have also been derived on the basis of alternative physical theories [4]. The method proposed here only assumes that such a relationship exists.

There are many circumstances where contact line motion is in some sense slow compared with the dynamics in the fluid's interior: droplet spreading [13]; flows on moderately inclined surfaces [2]; contact line motion restricted by pinning effects; motion initiated by slow external variation of wetting properties (e.g., electrowetting [40]). In this instance, the pressure is essentially constant, and the fluid's geometry can therefore be described as a "capillary" surface, a minimizer of surface and bulk energies subject to the constraint of a fixed contact line. This approximation, known as the quasisteady limit, was utilized first by Greenspan [16], and has appeared elsewhere [2,13,14,27,32,36]. Similar to what is presented here, Hocking and Miksis [19] used a boundary integral computation to study a ridge of fluid in the quasisteady limit.

Because the fluid geometry is entirely characterized by the contact line, the dynamic contact angle is a function of this curve alone. Together with the linearity of the minimization problem, this allows the evolution to be computed using integral equations along the curve (e.g. [1,22]). In contrast to PDE formulations, the computation only involves discretizing a curve instead of a two-dimensional domain. Furthermore, it will be shown that the resulting computational algorithm does not exhibit the stiffness problems intrinsic to high-order parabolic equations.

2. Problem formulation

If the motion of the contact line is in some sense slow compared to the rate at which capillary forces act, the fluid may be thought to be always in mechanical equilibrium. In the absence of body forces, the free-surface shape is therefore a minimizer of the liquid–vapor surface energy, subject to the constraint of a fixed contact line. A more precise discussion about the applicability of this quasi-steady assumption is presented in Appendix A.

In this paper, the fluid's free surface is assumed to be a graph $h(x,y)$. The function h has support Ω, whose boundary is the contact line Γ. In the small angle limit [6], the linearized contribution of surface energy is given by

$$\gamma \int_\Omega 1 + |\nabla h|^2 \mathrm{d}\mathbf{x}, \tag{2}$$

where γ is the liquid–vapor surface energy, which is presumed constant here. The minimizer of this expression, subject to the constraint of constant volume, is the quasi-steady droplet shape. Finding the minimizer amounts to solving the Euler–Lagrange problem

$$\Delta h = \lambda, \quad h|_\Gamma = 0, \quad \int h \,\mathrm{d}\mathbf{x} = M \equiv \text{volume}, \tag{3}$$

where λ is a Lagrange multiplier, which is essentially just the negative hydrostatic pressure.

The "apparent" contact angle θ is defined on the boundary of Ω (again in the small angle limit) as

$$\theta = -\frac{\partial h}{\partial \mathbf{n}}, \quad \mathbf{n} = \text{outward normal of } \Gamma. \tag{4}$$

The motion of Γ is then specified by prescribing the normal velocity, denoted V_n, as a function of this angle,

$$V_n = f(\theta; \theta_e, \mathbf{x}) = f(-\partial h/\partial \mathbf{n}; \theta_e, \mathbf{x}). \tag{5}$$

The function f can be any constitutive law relating the contact line velocity to the apparent contact angle θ and the equilibrium contact angle θ_e. Generally speaking, f is positive when $\theta > \theta_e$ and is an increasing function of θ. The spatial dependence of f may arise as a consequence of substrate inhomogeneities or other physical influences (see Section 3).

2.1. Integral equations

The Lagrange multiplier can be eliminated by the substitution,

$$w = \frac{h}{\lambda} - \frac{|x|^2}{4}, \tag{6}$$

so that w satisfies the boundary value problem,

$$\Delta w = 0, \quad w|_\Gamma = -\frac{|x|^2}{4}. \tag{7}$$

The normal derivative of w can be related to its boundary values by standard Green's function techniques. Letting

$$G(\mathbf{x}, \mathbf{x}_0) = \frac{1}{2\pi} \ln |\mathbf{x} - \mathbf{x}_0| \tag{8}$$

be the free-space Green's function for the Laplacian, one has the boundary integral equation,

$$\int_\Gamma w(\mathbf{x}) \frac{\partial G(\mathbf{x}, \mathbf{x}_0)}{\partial \mathbf{n}} - G(\mathbf{x}, \mathbf{x}_0) \frac{\partial w(\mathbf{x})}{\partial \mathbf{n}} \, ds(\mathbf{x}) = \frac{w(\mathbf{x}_0)}{2}, \quad \mathbf{x}_0 \in \Gamma. \tag{9}$$

With the aid of the divergence theorem, the volume conservation constraint can be written,

$$\begin{aligned} M &= \int_\Omega h \Delta \left(\frac{|\mathbf{x}|^2}{4} \right) d\mathbf{x} \\ &= \int_\Omega \Delta h \frac{|\mathbf{x}|^2}{4} d\mathbf{x} + \int_\Gamma \frac{1}{2} h \mathbf{x} \cdot \mathbf{n} - \frac{|\mathbf{x}|^2}{4} \frac{\partial h}{\partial \mathbf{n}} \, ds \\ &= \lambda \int_\Omega \frac{|\mathbf{x}|^2}{4} d\mathbf{x} - \int_\Gamma \frac{|\mathbf{x}|^2}{4} \frac{\partial h}{\partial \mathbf{n}} \, ds. \end{aligned} \tag{10}$$

Using (6), the identity $\nabla \cdot (|\mathbf{x}|^2 \mathbf{x}) = 4|\mathbf{x}|^2$ and the divergence theorem, this constraint takes the form of the boundary integral,

$$M = \lambda \int_\Gamma \frac{|\mathbf{x}|^2 \mathbf{x}}{16} - \frac{|\mathbf{x}|^2}{4} \left(\frac{\partial w}{\partial \mathbf{n}} + \frac{1}{2} \mathbf{x} \cdot \mathbf{n} \right) ds. \tag{11}$$

This allows λ to be computed from $\partial w/\partial \mathbf{n}$ only using information on the curve Γ.

2.2. Spatial discretization and approximation of integrals

The curve Γ is parameterized by arclength s, and is subdivided into n evenly spaced points $\mathbf{x}(s_i)$, $i = 0, \ldots, n-1$, where $s_i = iL/n$ and L is the total length of the curve. The second term of the integrand in (9) has a logarithmic singularity which must be dealt with carefully. This term can be split into singular and analytic parts as

$$G(\mathbf{x}(s), \mathbf{x}(s_0))f(\mathbf{x}(s)) = f(x(s))\left(\frac{1}{4\pi}\ln\left[4\sin^2\left(\frac{s-s_0}{2}\right)\right] + K_1(s, s_0)\right), \tag{12}$$

where $f(\mathbf{x}(s))$ has been identified with the normal derivative of w and

$$K_1(s, s_0) = \frac{1}{2\pi}\left\{\ln|\mathbf{x}(s) - x(s_0)| - \frac{1}{2}\ln\left[4\sin^2\left(\frac{s-s_0}{2}\right)\right]\right\}. \tag{13}$$

The integral of the logarithmic part is approximated using the spectrally accurate quadrature formula [25],

$$\int_0^L f(x(s))\ln\left[4\sin^2\left(\frac{s-s_i}{2}\right)\right]\mathrm{d}s = \frac{L}{2}\sum_{j=0}^{n-1} q_{|i-j|} f(x(s_j)), \tag{14}$$

where the weights are

$$q_j = -\frac{4}{n}\sum_{m=1}^{n/2-1}\frac{1}{m}\cos\frac{mj\pi}{n/2} - \frac{(-1)^j}{(n/2)^2}, \quad j = 0, \ldots, n-1. \tag{15}$$

We note that the kernel $\partial G(\mathbf{x},\mathbf{x}_0)/\partial\mathbf{n}$ is continuous along the curve Γ; in particular we have [15],

$$\frac{\partial G(\mathbf{x}(s), \mathbf{x}_0(s))}{\partial\mathbf{n}} \equiv K_2(s, s_0) = \begin{cases} \frac{1}{2\pi}\frac{(\mathbf{x}(s)-\mathbf{x}(s_0))\cdot\mathbf{n}}{|\mathbf{x}(s)-\mathbf{x}(s_0)|^2}, & s \neq s_0, \\ \frac{1}{4\pi}\kappa(s_0), & s = s_0, \end{cases} \tag{16}$$

where $\kappa(s_0)$ is the curvature of Γ at s_0. The trapezoid rule is used to evaluate the integrals involving K_1,K_2 as well as the integral in Eq. (11), giving spectral accuracy [37].

The result of all of this is that (9) is approximated by a dense, symmetric linear system in the unknowns $f_j \equiv \partial w/\partial\mathbf{n}(s_j)$ of the form,

$$\sum_{j=0}^{n-1}\left[\frac{Lq_{|i-j|}}{8\pi} + K_1(s_j, s_i)\right]f_j = -\frac{w(\mathbf{x}(s_i))}{2} + \sum_{j=0}^{n-1} K_2(s_j, s_i)w(\mathbf{x}(s_j)). \tag{17}$$

For the examples given below, this system is not large, and is solved efficiently using standard Cholesky factorization.

2.3. Time evolution

Once $\partial w/\partial\mathbf{n}$ is known, Eq. (11) is used to find λ. The contact angle is determined using (6), giving

$$\theta = -\lambda\left(\frac{\partial w}{\partial\mathbf{n}} + \frac{1}{2}\mathbf{x}\cdot\mathbf{n}\right), \tag{18}$$

from which the contact line velocity can be evaluated according to (5).

In contrast to other formulations of capillary driven fluid motions (e.g. [21]), this moving interface problem does not suffer from severe numerical stiffness. In Appendix B we show that a wavenumber k

perturbation to a circular interface has a decay rate $\sigma \sim -k$. This suggests that only a mild, CFL-type restriction on the timestep is necessary to achieve stability, and is verified by the numerical experiments we present below.

In addition to the normal interface velocity, an artificial tangential velocity V_t is constructed to maintain the equal arclength representation. Appendix C details how this velocity is computed. The gridpoints are updated according to the explicit scheme

$$\mathbf{x}(t + \Delta t) = \mathbf{x}(t) + \Delta t(V_n \mathbf{n} + V_t \mathbf{t}). \tag{19}$$

The tangent and normal vectors $\mathbf{t}$,$\mathbf{n}$ are found by spectral differentiation of $\mathbf{x}(s)$:

$$\mathbf{t} = \left(\frac{d\mathbf{x}}{ds}\right), \quad \mathbf{n} = \left(\frac{d\mathbf{x}}{ds}\right)^{\perp}. \tag{20}$$

The time step Δt is adapted to satisfy a constraint of the form

$$C_2 \Delta s \leqslant \Delta t \max |V_n| \leqslant C_1 \Delta s, \tag{21}$$

where the tolerances satisfy $C_2 < C_1 \ll 1$.

3. Computational results

The purpose of this section is to demonstrate qualitative phenomenon using the boundary integral method. We focus on several situations of interest: droplet spreading on homogeneous and heterogenous surfaces, topological transitions, and motion driven by heterogenous wetting. Gravitational effects will be considered in Section 4.

3.1. Spreading and relaxation dynamics

In the simplest case of a perfectly homogeneous substrate, many, but not all initial configurations will eventually obtain a circular shape. In the perfect-wetting case ($\theta_e = 0$), this solution will continue to spread forever, whereas in the partial wetting case ($\theta_e > 0$), a circular equilibrium will be reached. The other possible equilibria are multiple circular drops; these may result from droplet splitting, which we discuss in Section 3.3.

In the partially wetting case, a commonly used expression that relates the contact angle and speed is [7,41]

$$V_n = \theta^3 - \theta_e^3, \tag{22}$$

where θ_e is the equilibrium contact angle. Setting $\theta_e = 0$ reduces this to expression (1), corresponding to a perfectly wetting surface.

The computation in Fig. 1 shows a typical evolution of a drop into a convex, nearly circular drop. This drop continues to spread until the equilibrium radius

$$r_0 = \left(\frac{4M}{\pi\theta_e}\right)^{1/3} \tag{23}$$

is reached. Alternatively, growth of the circular interface on a perfectly wetting substrate will eventually follow the power law for the radius $r \sim t^{1/10}$ [5].

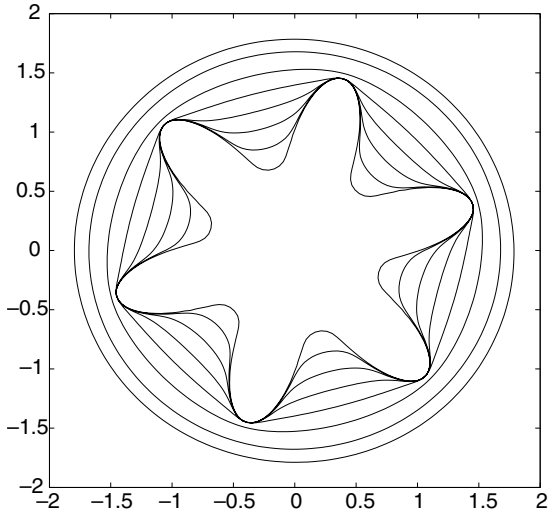

Fig. 1. Spreading of a non-convex fluid droplet ($\theta_e = 1$, $M = 4$). The contact line first approaches a circular shape, then spreads until equilibrium (the outer-most curve) is reached.

3.2. Flow around nonwetting defects

Everyday experience suggests that fluid contact lines frequently get stuck or "pinned" as a result of spatially localized surface defects. Such a defect can be modeled as a region R where contact line motion is prohibited. In a perfect wetting situation, a law incorporating this effect can be written

$$V_n = [1 - \chi_R]\theta^3, \tag{24}$$

where χ_R is the characteristic function of the set R.

Fig. 2 shows the evolution of the spreading fluid around a circular defect, with the same initial data as in section 3.1. Once the defect in encountered, spreading proceeds in a non-uniform fashion. Eventually the fluid will pass around the defect entirely, and the contact line will self-intersect. The numerical method makes no allowance for this to happen, although a scheme to reconnect the interface (see, e.g. [24]) could in principle be implemented to account for this.

3.3. Droplet splitting

Even without defects present, it is not clear that an irregular drop will always obtain a circular shape. Here we demonstrate that an initially connected region can develop a self-intersection. This initial configuration is a "dumbell" shape, just two circular drops connected by a thin neck (see Fig. 3). It should be pointed out that the symmetry here is somewhat important: if the circular regions on either side of the neck were substantially different sizes (i.e., different radii of curvature), they would have different pressures and the quasi-steady assumption leading to the original model would be violated.

The interfacial law assumed partial wetting: [10,13],

$$V_n = \theta(\theta^2 - \theta_e^2), \quad \theta_e = 0.7. \tag{25}$$

Other formulas describing partial wetting (e.g. (22)) appeared to give similar results.

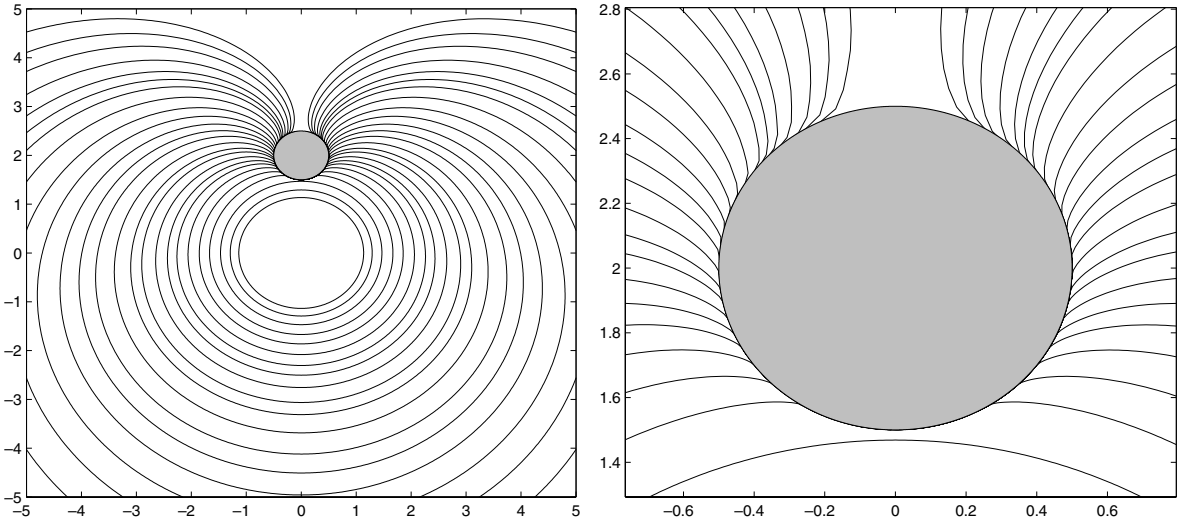

Fig. 2. Left: drop spreading around a non-wetting defect (512 gridpoints). Right: contact line motion near the defect.

Fig. 3 show the evolution of the drop. As the neck narrows, fluid is sucked into the circular regions. It eventually pinches at two different points along its length, generating self-intersections of Γ as in the previous example. One can speculate that the outcome is three drops: the two original ones and a "satellite" drop in the middle.

3.4. Heterogenous surface energies and droplet migration

Surface energies can vary spatially because of compositional differences, or because of imposed external fields. Drops will preferentially move to lower their solid–liquid and solid–vapor energies, which equivalently means that they will prefer to be on a more wettable surface with lower equilibrium contact angle. This is the dynamical mechanism which allows control of fluids by "electrowetting" phenomenon [40], for example.

This effect is incorporated here simply by adding a spatial dependence to the contact line law (22) of the form $\theta_e = \theta_e(\mathbf{x})$. In the example shown in Fig. 4, a drop is initially placed mostly on a surface with high contact angle, with some of the drop on a more wettable (low contact angle) surface. The drop attempts to reduce the area of its support on the high-contact angle surface by migrating to a lower energy surface. Eventually the entire drop lies on the surface of higher wettability.

4. Gravitational effects

The effects of gravity can be included in a straightforward manner in the quasi-steady model. The total energy is the sum of surface energy (2) and gravitational potential,

$$\int_\Omega \gamma(1+|\nabla h|^2) + g\rho\left(\frac{h^2}{2}+\sigma(\mathbf{x})h\right)\mathrm{d}\mathbf{x}, \tag{26}$$

where g is the gravitational acceleration and ρ is the fluid density. Topographical effects are specified by $\sigma(\mathbf{x})$, which designates the height of the underlying substrate. A non-dimensional description can be found by rescaling all lengths by the capillary length $\sqrt{\gamma/g\rho}$. The corresponding Euler–Lagrange problem is

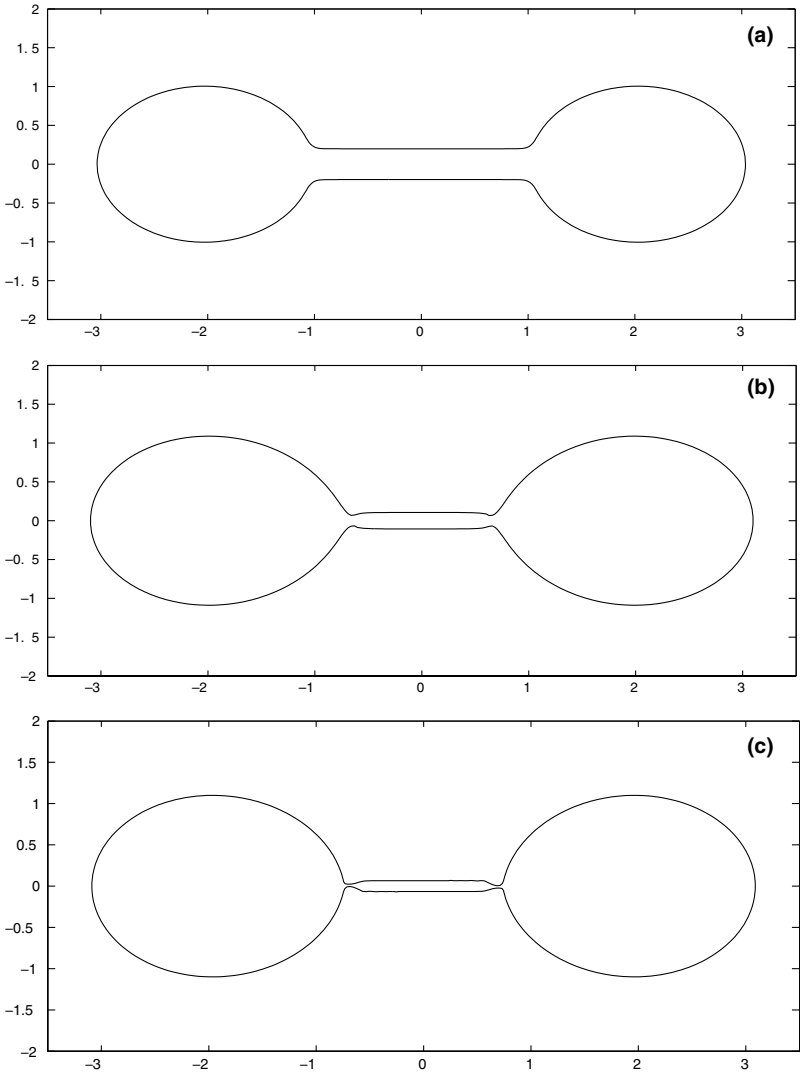

Fig. 3. Evolution of a thin neck of fluid (512 gridpoints). Two drops (a) are connected by a thin neck of fluid, pinching occurs close to each circular region (b), leading to splitting of the drop (c).

$$\Delta h - h = \lambda + \sigma(\mathbf{x}), \quad h|_\Gamma = 0, \quad \int h\,\mathrm{d}x = M. \tag{27}$$

In order to eliminate the inhomogeneous term, let $\Phi(\mathbf{x})$ be any function that satisfies

$$\Delta\Phi - \Phi = \sigma(\mathbf{x}). \tag{28}$$

The substitution $w = h - \Phi + \lambda$ gives the homogeneous problem,

$$\Delta w - w = 0, \quad w|_\Gamma = -\Phi + \lambda. \tag{29}$$

Let w_0,w_1 solve the two independent boundary value problems:

$$\Delta w_0 - w_0 = 0, \quad w_0|_\Gamma = -\Phi, \tag{30}$$

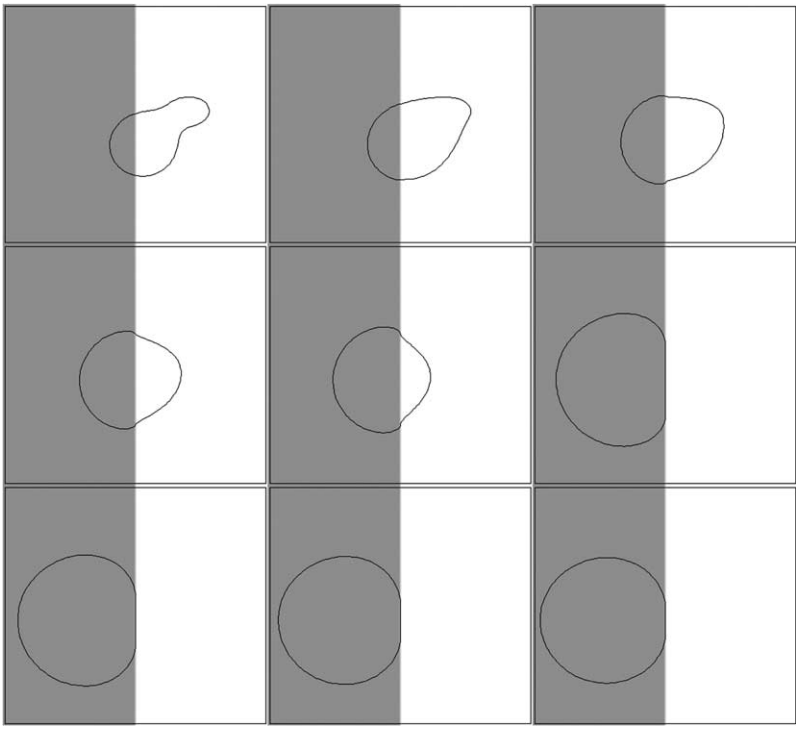

Fig. 4. Migration of a droplet from a surface of low wettability (white, $\theta_e = 1.5$) to a surface of high wettability (grey, $\theta_e = 0.5$).

$$\Delta w_1 - w_1 = 0, \quad w_1|_\Gamma = 1. \tag{31}$$

so that $w = w_0 + \lambda w_1$. The relationship between the mass constraint and the Lagrange multiplier can now be stated in terms of $\partial w_{0,1}/\partial \mathbf{n}$. For convenience, let $\mathbf{q}$ be some vector field whose divergence is Φ. Using 30,31, the definition of w and the divergence theorem,

$$\begin{aligned} M &= \int_\Omega w_0 + \Phi + \lambda(w_1 - 1)\mathrm{d}\mathbf{x} \\ &= \int_\Omega \Delta w_0 + \Phi + \lambda\Delta(w_1 - |\mathbf{x}|^2/4)\mathrm{d}\mathbf{x} \\ &= \int_\Gamma \left[\nabla w_0 + \mathbf{q} + \lambda(\nabla w_1 - \frac{1}{2}\mathbf{x})\right] \cdot \mathbf{n}\,\mathrm{d}s. \end{aligned} \tag{32}$$

Therefore λ is found as

$$\lambda = \frac{M - \int_\Gamma (\nabla w_0 + \mathbf{q}) \cdot \mathbf{n}\,\mathrm{d}s}{\int_\Gamma (\nabla w_1 + \frac{1}{2}\mathbf{x}) \cdot \mathbf{n}\,\mathrm{d}s}. \tag{33}$$

4.1. Integral equations

To solve for the normal boundary derivatives corresponding to equations (30) or (31), one has the boundary integral equation

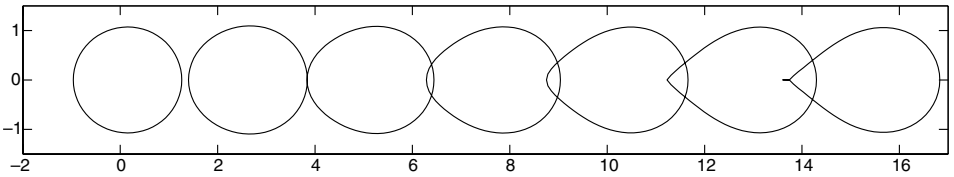

Fig. 5. Evolution of a drop (from left to right) on an inclined surface (slope = 0.6) showing the formation of a cusp. The right-most droplet's contact line exhibits unphysical self-intersection.

$$\int_\Gamma w(\mathbf{x})\frac{\partial G(\mathbf{x},\mathbf{x}_0)}{\partial \mathbf{n}} - G(x,x_0)\frac{\partial w(\mathbf{x})}{\partial \mathbf{n}}\,\mathrm{d}s = \frac{w(\mathbf{x}_0)}{2}. \tag{34}$$

The Green's function in this case is $G = (1/2\pi)K_0(|\mathbf{x} - \mathbf{x}_0|)$, where K_0 is the modified Bessel function of the second kind. The kernel $K_0(r)$ has a logarithmic singularity akin to (8), and is treated using the same quadrature formulas as discussed in Section 2.2. The other numerical details are also similar.

4.2. Flow on an inclined plane: cusp formation

Recent experimental [31] and theoretical [2,38] studies have demonstrated that a droplet subjected to gravitational forces may develop a contact line with a cusp at the fastest receding point. As an example, consider a drop sliding on an inclined plane with slope α, described by the substrate height function $\sigma(x,y) = -\alpha x$. The corresponding auxiliary functions Φ, $\mathbf{q}$ are

$$\Phi = \alpha x, \quad \mathbf{q} = \frac{1}{2}\alpha x^2 \mathbf{i}. \tag{35}$$

For a contact line law, we use (22) with equilibrium contact angle $\theta_e = 1$. The initial circular drop (radius 1, $M = 0.5$) both spreads and slides to the right. Fig. 5 shows the progression of the circular drop to one which is has a cusp of finite angle on the trailing edge. It should be noted that past the point at which the cusp forms, the numerical contact line self-intersects.

5. Conclusions

A versatile procedure for computing dynamical fluid wetting phenomenon has been presented. While the quasi-steady model employed is only approximate, the gain in computational efficiency makes this method attractive in contrast to two-dimensional PDE computations. The main drawback is the necessity of solving dense, linear systems. For large problems (>1000 unknowns) this can be accomplished efficiently, however, using a combination of iterative and fast-multipole methods [15].

The computational results here suggest a number of challenging problems reserved for future work. Included among them are the specific roles played by surface inhomogeneities, the formation of non-smooth irregularities such as cusps, and incorporating non-steady corrections into the present approximation. One could also consider the dynamics of dewetting films by solving an exterior Laplacian problem, as done in [26].

Acknowledgement

The author has benefited from discussions on boundary integral methods with Vladimir Ajaev. This work was partially supported under NSF award DMS-0405596.

Appendix A. Justification of the quasi-steady limit

We can formally derive a condition for when the quasi-steady assumption is valid by dimensional analysis. In the interior of the fluid droplet, capillary relaxation will proceed according to the lubrication equation (e.g. [9])

$$h_t = \gamma/3\mu\nabla\cdot(h^3\nabla\Delta h),$$

where μ is the viscosity. Let W,H be the typical scales for width and height of a droplet. Nondimensionalize by rescaling

$$x = Wx'; \quad h = Hh'; \quad t = \tau_c t'. \tag{36}$$

The natural timescale for capillary relaxation τ_c can be defined in a way so that the resulting non-dimensionalized equation is free of parameters by setting

$$\tau_c = \frac{W^4}{H^3}\gamma/3\mu,$$

leading to

$$H_{t'} = \nabla\cdot(H^3\nabla\Delta H).$$

If V_l is the typical contact line velocity, the timescale for contact line movement is, with respect to the same rescaling

$$\tau_l = \frac{W}{V_l}. \tag{37}$$

For capillary relaxation to dominate, one needs $\tau_c \ll \tau_l$ which is the same as

$$\frac{V_l}{\gamma/3\mu} \ll \alpha^3, \quad \alpha = \frac{H}{W} = \text{aspect ratio}.$$

The quantity on the left is the capillary number Ca. Under certain circumstances [13] one can show that Ca is moderately small independent of the geometry, in the sense that is scales with a microscopic parameter ϵ as $Ca \sim \mathcal{O}(1/\ln\epsilon^{-1})$.

Appendix B. Linear analysis of a circular interface

We suppose here that the contact line law $f(\theta)$ which admits an equilibrium $f(\theta_e) = 0$. An equilibrium drop of radius r_0 in polar coordinates (r,ϕ) has the shape described by

$$h_0(r,\phi) = A(1-(r/r_0)^2), \quad A = \frac{1}{2}r_0\theta_e.$$

Suppose that the contact line's position is given by the graph $r = \eta(\phi,t)$, and is subject to the perturbation

$$\eta = r_0 + \epsilon e^{\sigma t}\cos k\phi, \quad k = 1,2,3,\ldots$$

Expanding the droplet shape as $h = h_0 + \epsilon h_1 + \cdots$ and the Lagrange multiplier in (3) in a similar way, the leading order perturbation h_1 satisfies

$$\Delta h_1 = \lambda_1, \quad \int_\Omega h_1 \mathrm{d}A = 0, \quad h_1(r_0,\phi) = \theta_e e^{\sigma t}\cos k\phi.$$

The solution to this constrained boundary value problem is

$$h_1 = \theta_e (r/r_0)^k e^{\sigma t} \cos k\phi.$$

Expanding the normal derivative in powers of ϵ,

$$\begin{aligned}\frac{\partial h}{\partial n}(\eta,\phi) &= -\theta_e + \epsilon\left(\frac{\partial h_1}{\partial n}(r_0,\phi) + \frac{\partial^2 h_0}{\partial n^2}(r_0,\phi)e^{\sigma t}\cos k\phi\right) + \mathcal{O}(\epsilon^2)\\ &= -\theta_e + \epsilon[(k-1)\theta_e/r_0]e^{\sigma t}\cos k\phi + \mathcal{O}(\epsilon^2).\end{aligned}$$

At order ϵ, the normal velocity is then

$$\sigma e^{\sigma t}\cos k\phi = f(-\partial h/\partial n) = -[(k-1)f'(\theta_e)\theta_e/r_0]e^{\sigma t}\cos k\phi,$$

so that

$$\sigma = -(k-1)f'(\theta_e)\theta_e/r_0.$$

The neutrally growing mode $k = 1$ is just a translation of the drop; the other modes decay at the moderate rate $\sigma \sim -k$.

Appendix C. Computation of the tangential velocity

Let $\mathbf{x}_i$ be the ith gridpoint, and identify $\mathbf{x}_n$ with $\mathbf{x}_0$. The curve Γ is evolved according to (19) using the normal V_n and tangential V_t velocity components. Given V_n, we need to find the tangential velocity $V_i \equiv V_t(x_i)$ which maintains the constraint of equal spacing

$$|\mathbf{x}_{i+1}(t+\Delta t) - \mathbf{x}_i(t+\Delta t)|^2 = C, \quad 1 \leqslant i \leqslant n,$$

where C is an unknown constant. Letting $\mathbf{z} = \mathbf{x}(t) + \Delta t V_n \mathbf{n}$ and using (19), this amounts to solving the weakly nonlinear problem,

$$2(\mathbf{z}_{i+1} - \mathbf{z}_i)\cdot(V_{i+1}\mathbf{t}_{i+1} - V_i\mathbf{t}_i) = -|\mathbf{z}_{i+1} - \mathbf{z}_i|^2 - |V_{i+1}\mathbf{t}_{i+1} - V_i\mathbf{t}_i|^2 + C, \quad 1 \leqslant i \leqslant n,$$

where $\mathbf{t}_i$ is the tangent vector at x_i. Subtracting the ith and $(i-1)$th equations eliminates C and gives

$$\begin{aligned}&(\mathbf{z}_{i+1} - \mathbf{z}_i)\cdot\mathbf{t}_{i+1}V_{i+1} + (\mathbf{z}_i - \mathbf{z}_{i-1})\cdot\mathbf{t}_{i-1}V_{i-1} - (\mathbf{z}_{i+1} - \mathbf{z}_{i-1})\cdot\mathbf{t}_i V_i\\ &\quad = -\frac{1}{2}[|\mathbf{z}_{i+1} - \mathbf{z}_i|^2 - |\mathbf{z}_i - \mathbf{z}_{i-1}|^2 + |V_{i+1}\mathbf{t}_{i+1} - V_i\mathbf{t}_i|^2 - |V_i\mathbf{t}_i - V_{i-1}\mathbf{t}_{i-1}|^2], \quad 1 \leqslant i \leqslant n.\end{aligned}$$

The left hand side is linear in V, and the whole system can be solved efficiently by iteration.

References

[1] V.S. Ajaev, S.H. Davis, Boundary-integral simulations of containerless solidification, J. Comp. Phys. 187 (2003) 492–503.
[2] M. Ben Amar, L. Cummings, Y. Pomeau, Points singuliers d'une ligne de contact mobile, C.R. Acad. Sci. Paris 329 (2001) 277–282.
[3] M. Bertsch, R. Dal Passo, S.H. Davis, L. Giacomelli, Effective and microscopic contact angles in thin film dynamics, Eur. J. Appl. Math. 11 (2000) 181–201.
[4] T.D. Blake, J.M. Haynes, Kinetics of liquid/liquid displacement, J. Colloid Interf. Sci. 30 (1969) 421–423.
[5] M. Brenner, A. Bertozzi, Spreading of droplets on a solid surface, Phys. Rev. Lett. 71 (1993) 593–596.
[6] A. Cameron, Principles of Lubrication, Longmans, London, 1966.
[7] R.G. Cox, The dynamics of the spreading of liquids on a solid surface. Part 1. Viscous flow, J. Fluid Mech. 168 (1986) 169–194.
[8] R.G. Cox, Inertial and viscous effects on dynamic contact angles, J. Fluid Mech. 357 (1998) 249–278.

[9] P.G. de Gennes, Wetting: statics and dynamics, Rev. Mod. Phys. 57 (1985) 827.
[10] P.G. de Gennes, Deposition of langmuir-blodgett layers, Colloid Polym. Sci. 264 (1986) 463–465.
[11] J.B. Freund, The atomic detail of a wetting/dewetting flow, Phys. Fluids 15 (2003) L33.
[12] K. Glasner, Nonlinear preconditioning for diffuse interfaces, J. Comp. Phys. 174 (2001) 695–711.
[13] K.B. Glasner, Spreading of droplets under the influence of intermolecular forces, Phys. Fluids 15 (2003) 1837–1842.
[14] K.B Glasner, Variational models for moving contact lines and the quasi-static approximation (2004), preprint.
[15] A. Greenbaum, L. Greengard, G.B. McFadden, Laplace's equation and the Dirichlet–Neumann map in multiply connected domains, J. Comput. Phys. 105 (1993) 267–278.
[16] H.P. Greenspan, On the motion of a small viscous droplet that wets a surface, J. Fluid Mech. 84 (1978) 125–143.
[17] G. Grun, M. Rumpf, Simulations of singularities and instabilities arising in thin film flow, Eur. J. Appl. Math. 12 (2001) 293–320.
[18] N.G. Hadjiconstantinou, Hybrid atomistic-continuum formulations and the moving contact line problem, J. Comp. Phys. 154 (1999) 245–265.
[19] L.M. Hocking, M.J. Miksis, Stability of a ridge of fluid, J. Fluid Mech. 247 (1993) 157–177.
[20] L.M. Hocking, A.D. Rivers, J. Fluid Mech. 121 (1982) 425.
[21] T.Y. Hou, J.S. Lowengrub, M.J. Shelley, Removing the stiffness from interfacial flows with surface tension, J. Comp. Phys. 114 (1994) 312.
[22] T.Y. Hou, J.S. Lowengrub, M.J. Shelley, Boundary integral methods for multicomponent fluids and multiphase materials, J. Comput. Phys. 169 (2001) 302–362.
[23] C. Huh, L.E. Scriven, Hydrodynamic model of steady movement of a solid/liquid/fluid contact line, J. Colloid Interf. Sci. 35 (1971) 85–101.
[24] D. Juric, G. Tryggvason, A front tracking method for dendritic solidification, J. Comp. Phys. 123 (1996) 127.
[25] R. Kress, On the numerical solution of a hyper-singular integral equation in scattering theory, J. Comp. Appl. Math. 61 (1995) 345–360.
[26] P.G. Lopez, M.J. Miksis, S.G.S. Bankoff, Stability and evolution of a dry spot, Phys. Fluids 13 (2001) 1601–1614.
[27] V.S. Nikolayev, D.A. Beysens, Relaxation of nonspherical sessile drops towards equilibrium, Phys. Rev. E 65 (2002) 046135.
[28] A. Oron, S.G. Bankoff, Dynamics of a condensing liquid film under conjoining/disjoining pressures, Phys. Fluids 13 (2001) 1107–1117.
[29] A. Oron, S.H. Davis, S.G. Bankoff, Long-scale evolution of thin liquid films, Rev. Mod. Phys. 69 (1997) 931–980.
[30] L. Pismen, Y. Pomeau, Nonlocal diffuse interface theory of thin films and the moving contact line, Phys. Rev. E 62 (2000) 2840.
[31] T. Podgorski, J.-M. Flesselles, L. Limat, Corners, cusps and pearls in running drops, Phys. Rev. Lett. 87 (2001) 036102.
[32] Y. Pomeau, Recent progress in the moving contact line problem: a review, C.R. Acad. Sci. 330 (2002) 207–222.
[33] L. Schwartz, Unsteady Simulation of Viscous Thin-layer Flows, Computational Mechanics Publications, Boston, 1997, pp. 203–233.
[34] L.W. Schwartz, R.V. Roy, R.R. Eley, S. Petrash, Dewetting patterns in a drying liquid film, J. Colloid Interf. Sci. 234 (2001) 363–374.
[35] P. Seppecher, Moving contact lines in the Cahn–Hilliard theory, Int. J. Eng. Sci. 34 (1996) 977–992.
[36] Y.D. Shikhmurzaev, Spreading of drops on solid surfaces in a quasi-static regime, Phys. Fluids 9 (1997) 266.
[37] A. Sidi, M. Israeli, Quadrature methods for singular and weakly fredholm integral equations, J. Sci. Comp. 3 (1988) 201–231.
[38] H. Stone, L. Limat, S. wilson, J.-M. Flesselles, T. Podgorski, Gingularite angulese d'nue ligne de contact en mouvement sur un subsrat solide, C.R. Physique 103 (2002) 103–110.
[39] L. Tanner, The spreading of silicone oil drops on horizontal surfaces, J. Phys. D 12 (1979) 1473–1484.
[40] H.J.J. Verheijen, M.W.J. Prins, Reversible electrowetting and trapping of charge: model and experiments, Langmuir 15 (1999) 6616–6620.
[41] O.V. Voinov, Hydrodynamics of wetting (English translation), Fluid Dynam. 11 (1976) 714–721.
[42] D.E. Weidner, L.W. Schwartz, Contact-line motion of shear-thinning liquids, Phys. Fluids 6 (1994) 3535.
[43] L. Zhornitskaya, A.L. Bertozzi, Positivity perserving numerical schemes for lubrication-type equations, SIAM J. Numer. Anal. 37 (2000) 523–555.